Modular degradable dendrimers enable small RNAs to extend survival in an aggressive liver cancer model

Kejin Zhou[a,b,1], Liem H. Nguyen[c,d,e,1], Jason B. Miller[a,b], Yunfeng Yan[a,b], Petra Kos[a,b], Hu Xiong[a,b], Lin Li[c,d,e], Jing Hao[a,b], Jonathan T. Minnig[a,b], Hao Zhu[c,d,e], and Daniel J. Siegwart[a,b,2]

[a]Simmons Comprehensive Cancer Center, The University of Texas Southwestern Medical Center, Dallas, TX 75390; [b]Department of Biochemistry, The University of Texas Southwestern Medical Center, Dallas, TX 75390; [c]Children's Research Institute, The University of Texas Southwestern Medical Center, Dallas, TX 75390; [d]Department of Pediatrics, The University of Texas Southwestern Medical Center, Dallas, TX 75390; and [e]Department of Internal Medicine, The University of Texas Southwestern Medical Center, Dallas, TX 75390

Edited by Robert Langer, Massachusetts Institute of Technology, Cambridge, MA, and approved November 30, 2015 (received for review October 22, 2015)

RNA-based cancer therapies are hindered by the lack of delivery vehicles that avoid cancer-induced organ dysfunction, which exacerbates carrier toxicity. We address this issue by reporting modular degradable dendrimers that achieve the required combination of high potency to tumors and low hepatotoxicity to provide a pronounced survival benefit in an aggressive genetic cancer model. More than 1,500 dendrimers were synthesized using sequential, orthogonal reactions where ester degradability was systematically integrated with chemically diversified cores, peripheries, and generations. A lead dendrimer, 5A2-SC8, provided a broad therapeutic window: identified as potent [EC_{50} < 0.02 mg/kg siRNA against FVII (siFVII)] in dose–response experiments, and well tolerated in separate toxicity studies in chronically ill mice bearing *MYC*-driven tumors (>75 mg/kg dendrimer repeated dosing). Delivery of *let-7g* microRNA (miRNA) mimic inhibited tumor growth and dramatically extended survival. Efficacy stemmed from a combination of a small RNA with the dendrimer's own negligible toxicity, therefore illuminating an underappreciated complication in treating cancer with RNA-based drugs.

dendrimers | miRNA | cancer

Since the discovery of RNAi and the recognition of its therapeutic potential, there has been a continuous search for optimal delivery carriers (1–10). Tremendous progress has been made with regard to delivery efficacy of small RNAs to healthy livers, but the clinically required combination of high delivery potency to tumors and low hepatotoxicity is not currently met by existing delivery vehicles. This challenge represents an unappreciated complication in treating cancer with RNA-based drugs. Primary liver cancer, a chronic consequence of liver cirrhosis, is a leading cause of cancer death and a major global health problem (11). Unfortunately, all five phase III human clinical trials of small-molecule drugs for hepatocellular carcinoma (HCC) treatment failed within the past four years in part because debilitating, late-stage liver dysfunction amplifies drug toxicity (11, 12). MicroRNAs (miRNAs) present a promising alternative cancer treatment strategy because they can function as tumor suppressors by concurrently targeting multiple pathways involved in cell differentiation, proliferation, and survival (13–19). In this study, we used a highly aggressive, inducible *MYC*-driven transgenic liver cancer model where the chance for successful therapy is very limited, in equal part due to the rapidly growing cancer and the compromised function of the overtaken liver. Tumors grow endogenously from within the liver in this genetically engineered model, which is biologically faithful and lethal, in contrast to standard xenograft or orthotopic models derived from cell line implantation (20). The development of dendrimer carriers that can mediate a therapeutic benefit in this difficult-to-treat model was set as the paramount goal of the study. Notably, we find that high potency and low toxicity are of critical importance in the context of aggressive liver cancer models, where the carrier's own toxicity can negate the benefit of on-target small-RNA therapies.

To achieve this balance of low toxicity and high potency, we reasoned that one must more precisely examine the influence of chemical structure by expanding the structural diversity and molecular size of delivery carriers. Dendrimers represented an ideal system for this goal because they possess the same high degree of molecular uniformity as small molecules and the broad theoretical space for chemical tuning as polydisperse polymers (21–23). These intrinsic characteristics enable dendrimers to have unique properties for various biomedical applications (24–26). In gene delivery, most studies have used the limited number of commercial dendrimers for further chemical modification (27–29). However, orthogonal click chemistry has recently made a transformative impact on the synthesis of dendritic materials through protecting group-free methodologies to overcome historical limitations in fidelity and provide a larger toolbox for dendrimer design (30–34). The expansion of dendrimer applications therefore depends on the ability to easily tune the size, chemistry, topology, and, ultimately, dendrimer physical properties through chemical synthesis.

We hypothesized that, through introduction of ester bonds and molecular diversity at each expansion step, modular degradable dendrimers would possess a critical balance of low toxicity and high delivery potency (Fig. 1). We further speculated that chemical modulation of cores, peripheries, and generations may be accelerated by utilization of efficient click reactions to enable a large increase in both the total number (>1,500) and

Significance

Liver cancer is a leading cause of death and a global health problem. Unfortunately, five small-molecule drugs for hepatocellular carcinoma (HCC) recently failed phase III clinical trials partly because late-stage liver dysfunction amplifies drug toxicity. MicroRNAs (miRNAs) present a promising alternative treatment strategy but require development of delivery vehicles that can avoid this cancer-induced dysfunction, which exacerbates toxicity. We overcame this challenge by developing dendrimer nanoparticles that mediate miRNA delivery to late-stage liver tumors with low hepatotoxicity. An aggressive, *MYC*-driven transgenic liver cancer model was used to examine *let-7g* tumor suppressor efficacy, resulting in a significant survival benefit. These dendrimer carriers provide high potency in tumors without negatively affecting normal tissues, solving a critical issue in treating aggressive liver cancer.

Author contributions: K.Z. and D.J.S. designed research; K.Z., L.H.N., J.B.M., Y.Y., P.K., L.L., and D.J.S. performed research; H.Z. and D.J.S. supervised research; K.Z., J.B.M., Y.Y., H.X., J.H., J.T.M., and D.J.S. contributed new reagents/analytic tools; K.Z., L.H.N., H.Z., and D.J.S. analyzed data; and K.Z. and D.J.S. wrote the paper.

The authors declare no conflict of interest.

This article is a PNAS Direct Submission.

[1]K.Z. and L.H.N. contributed equally to this work.

[2]To whom correspondence should be addressed. Email: daniel.siegwart@utsouthwestern.edu.

This article contains supporting information online at www.pnas.org/lookup/suppl/doi:10.1073/pnas.1520756113/-/DCSupplemental.

www.pnas.org/cgi/doi/10.1073/pnas.1520756113

chemical diversity of dendrimers. Biocompatible, degradable esters were included as a key design component because all RNAi therapies are transient and require sustained and repeated treatment. This ultimately enabled discovery of well-tolerated small-RNA carriers that could produce a therapeutic benefit in a challenging liver cancer model.

Efficacious delivery requires overcoming a series of extracellular and intracellular barriers (1). The physicochemical properties of small RNAs (high molecular weight, anionic charge, and hydrophilic nature) prevent passive diffusion across cell membranes. Studies of lipid and polymer carriers have implicated at least two common elements: chemical groups to bind small RNAs and nanoparticle (NP)-stabilizing hydrophobicity, which combine to encapsulate RNA molecules inside stable NPs and release small RNAs into the cytosol after endocytosis (35). Particular tertiary amines with optimal pK_a, alkyl chains, and defined topology/structure have been identified in effective carriers (2–10, 35–37).

Despite these advances, demonstration of effective survival benefit in aggressive genetic models of human cancer has not been achieved with synthetic carriers due to the lack of delivery vehicles that avoid cancer-induced organ dysfunction. To address this, we designed a dendrimer library organized through binding, stabilization, and chemical functionality within the cores and peripheries. In vitro and in vivo evaluation identified dendrimers with optimal topological structures and high delivery efficacy (EC_{50} of FVII knockdown < 0.02 mg/kg). Structure–activity knowledge was used to rationally design additional carriers with predicted in vivo activity. Evaluation of lead dendrimer candidates identified **5A2-SC8** as exhibiting low toxicity after repeated 75 mg/kg dendrimer i.v. dosing in chronically ill, tumor-bearing mice. Finally, we demonstrate that **5A2-SC8** can deliver a *let-7g* tumor suppressor miRNA with high in vivo potency to suppress tumor growth and result in a dramatic survival benefit of transgenic mice bearing aggressive, *MYC*-driven liver cancer. These findings suggest that modular degradable dendrimers may greatly expand the scope of chemical discovery research for therapeutic dendrimer delivery applications, ultimately providing new avenues for development of RNA cancer treatments by expansion of the therapeutic window.

Results

A Modular Synthesis Strategy Allowed Diversification in the Chemical Functionality and Molecular Weight of Ester-Based Dendrimer Carriers. Liver cancer is a challenging host for therapeutic intervention because drug-induced hepatotoxicity can exacerbate the underlying liver disease (12). Therefore, to achieve effective RNAi-mediated therapy, a balance of high potency and low toxicity of the carrier has to be maintained. This requires a versatile chemical synthesis strategy to easily tune the delivery carrier in terms of molecular weight, chemical structure, and ultimate physical properties (Fig. 2). Motivated by recent methodology developments in orthogonal click chemistry (30–34), we envisioned that efficient sequential reactions could accelerate dendrimer synthesis, thereby allowing systematic fine-tuning of small-RNA binding affinity and NP-stabilizing hydrophobicity of dendrimer carriers. Particularly, the use of asymmetric monomers was reported as an effective strategy to construct polyester dendrimers with a series of generations (33). Inspired by that methodology, we investigated the feasibility of sequential aza- and sulfa-Michael additions to 2-(acryloyloxy)ethyl methacrylate (AEMA) as a strategy to synthesize a degradable dendrimer library with enough chemical diversity to solve the delivery challenge to vulnerable cancerous hosts.

Before attempting to synthesize a library of dendrimers, we had to first verify that the asymmetric AEMA method is capable of yielding diverse dendrimers using a variety of chemically distinct amine and thiol compounds. Quantitative reaction conversion and high tolerance of different amine/thiol functionalities is required to synthesize monodisperse dendrimers and ensure accurate small-RNA delivery results. To examine the robustness of this chemistry, we chose the most difficult starting materials, tris(2-aminoethyl)amine with six N–H bonds and tetradecylamine with a 14-carbon-length alkyl chain to test structural limits of the orthogonal Michael addition reactions. Both tris(2-aminoethyl)amine and tetradecylamine could quantitatively and selectively react with the acrylate functionality in AEMA after 24 h in the presence of 5 mol% of butylated hydroxytoluene (to inhibit radical formation) at 50 °C, whereas AEMA by itself remained unreacted under these conditions (*SI Appendix*, Figs. S1 and S2). Next, we focused on 2-(butylamino)ethanethiol and 1-tetradecanethiol to test sulfa-Michael addition. Using the established aza-Michael addition conditions (DMSO as solvent without any catalyst), conversion of 1-tetradecanethiol was less than 80% (*SI Appendix*, Figs. S3 and S4). To achieve quantitative conversion, we screened a series of catalysts and conditions to improve the reaction conversion. Ultimately, dimethylphenylphosphine (DMPP) was found to be an effective a catalyst to achieve the final products under reaction at low concentration (≥125 mM), small scale (~20 mg on average), and in high conversion (100% by ^{1}H NMR) (*SI Appendix*, Figs. S3 and S4).

We then used the optimized sequential aza- and sulfa-Michael reactions to react with ester-based AEMA to construct a chemically diversified library of degradable dendrimers through various parameters: core (**C**), linkage (**L**), and periphery (**P**) (Fig. 2). We initially evaluated the effects of small-RNA binding affinity and NP-stabilizing hydrophobicity of dendrimer carriers by reacting 42 core-forming amines **C** and 36 periphery-modifying thiols **P** to generate a 1,512 first-generation (G1) dendrimer library. The resulting compounds possessed diversity in the chemical composition and number of branches. We chose esters as the key degradable linkage (**L**) because polyesters are used in Food and Drug Administration-approved drug delivery products with minimal toxicity (38). At each dendrimer growth step, the ester number increases, which provides an opportunity to identify degradable dendrimers with balanced potency and toxicity. The library was established effectively with high purity (*SI Appendix*, Fig. S5). Concurrent delivery efficacy results allowed for optimization during the synthesis process (*SI Appendix*, Fig. S6). In particular, structure–activity relationships (SARs) that emerged allowed for the rational design of higher-generation dendrimers with predicted activity to validate our approach. We prepared multibranched dendrimers by choosing polyamines with five or six NH bonds (such as natural amines, spermidine, and spermine). We synthesized higher-generation (G2 to G4) dendrimers via generation expansion reactions (*SI Appendix*, Fig. S7), starting from lower branching amine cores. This process successfully allowed us to take amine cores that were inactive in the in vitro screen, and then rationally design higher-generation dendrimers with in vivo activity. All lead dendrimers were resynthesized in larger scale and purified by flash chromatography before conducting in vivo studies.

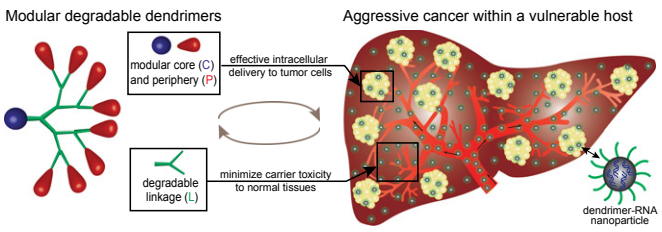

Fig. 1. RNA-based liver cancer therapies are hindered by the lack of potent and nontoxic delivery vehicles that avoid late-stage liver dysfunction that exacerbates toxicity. We envisioned that a modular design would allow discovery of dendrimers that balance low hepatotoxicity and high in vivo small-RNA delivery potency to tumor cells by fine-tuning of the identity and position of functional groups within dendrimer architectures.

Degradable Dendrimers Can Overcome Extracellular and Intracellular Barriers to Enable Delivery. We first identified which dendrimers can mediate siRNA to overcome intracellular barriers by screening

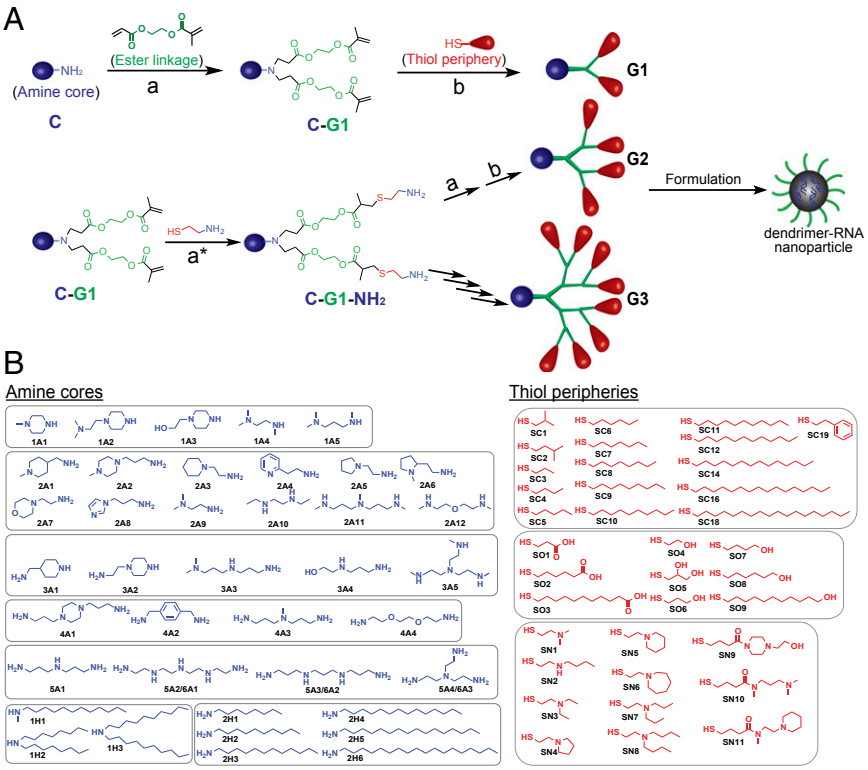

Fig. 2. A modular strategy for diversifying the chemical functionality and size of ester-based dendrimers allowed discovery of potent and nontoxic dendrimers for in vivo small-RNA delivery to tumor cells. (*A*) Orthogonal reactions accelerated the synthesis of >1,500 modular degradable dendrimers by combination of 42 cores (**C**) and 36 peripheries (**P**) through degradable linkages (**L**) and generations. The library was established via sequential reactions. First, amines (**C**) with a series of N–H bonds reacted quantitatively and selectively with the less steric acrylate groups of AEMA (**L**). The products (**C–L**) then quantitatively reacted with various thiols (**P**) under optimized DMPP-catalyzed conditions. (*B*) Dendrimers were independently modulated with chemically diverse amines and thiols. Selected amines were divided into two categories: ionizable amines (1A–6A) to tune RNA binding from **C** that generated one to six branched dendrimers, and alkyl amines (1H–2H) to tune NP **C** stabilization. Alkyl thiols (SC1–SC19) and alcohol/carboxylic acid terminated thiols (SO1–SO9) were selected to tune NP **P** stabilization. Aminothiols (SN1–SN11) were selected to tune **P** RNA binding. G2–G4 higher-generation dendrimers with multiple branches were also synthesized using generation expansion reactions (*SI Appendix*, Fig. S7).

the 1,512 member library for the ability to deliver siRNA in vitro to HeLa cells that stably expressed luciferase. Dendrimers were formulated into NPs containing luciferase-targeting siRNA (siLuc) and the helper lipids cholesterol, 1,2-distearoyl-*sn*-glycero-3-phosphocholine (DSPC), and lipid PEG2000 (3, 4). Intracellular delivery potential was assessed by quantifying reduction of luciferase expression without affecting cell viability (Fig. 3*A*). Eighty-eight hits were identified that mediated >50% knockdown of luciferase activity, which corresponded to a 6% hit rate across the entire library. The heat map was divided into structural zones and analyzed further based on branch type, number, and length (*SI Appendix*, Fig. S6). We found that dendrimers with an siRNA-binding core and a NP-stabilizing periphery had much higher intracellular siRNA delivery potential. Hydrophobic stabilization from the dendrimer periphery likely results in increased hydrophobic packing that provides additional NP stability (39). Further examination of branch number and branch lengths revealed that dendrimers with a binding core and three to six **SC5-SC12** branches have >25% chance to deliver siLuc into HeLa cells with >50% luciferase knockdown (*SI Appendix*, Fig. S6).

Having identified dendrimers that can overcome intracellular barriers, we next identified the dendrimers that can also overcome extracellular barriers to deliver siRNA in vivo. We selected 50 G1–G4 dendrimers based on in vitro delivery efficacy and SAR analysis, aiming to maximize chemical diversity. We evaluated dendrimers for their ability to silence Factor VII (FVII) in hepatocytes because this blood-clotting factor can be readily quantified from a small serum sample (3, 4). Dendrimers were formulated with an siRNA against FVII (siFVII) and were injected i.v. into mice at a dose of 1 mg/kg siRNA. FVII activity was quantified 3 d postinjection. We found that the most potent G1 dendrimers for in vivo delivery contained a binding core and four to six branches with **SC8-12** periphery composition (Fig. 3*B*). Interestingly, the optimal carriers for in vivo liver delivery were lower-generation (G1) dendrimers that have structural similarity to lipidoids (2, 3). Within formulated NPs that contain DSPC, cholesterol, and lipid PEG, there may be structural and size limitations to optimal packing within the NP morphology (39). Nevertheless, higher-generation dendrimers of **1A2**, **2A2**, and **3A3** and **3A5** with four to six **SC** branches did demonstrate improved siRNA delivery compared with their lower-branch number precursors, suggesting ways to rationally design and improve carriers. Dendrimers with eight branches were less active, further validating the established SAR information that the most potent dendrimers contain an amine-rich binding core and four to six **SC8-SC12** branches. We also measured the apparent pK_a of the formulated NPs using the 2-(*p*-toluidino)-6-napthalene sulfonic acid assay (TNS) (8). Lead dendrimers possessed an apparent pK_a between 6.3 and 6.6 (*SI Appendix*, Fig. S8), which is in good agreement with other studies of lipid and lipidoid NPs (8–10).

To further understand in vivo siRNA delivery to the liver, we studied biodistribution and in vivo knockdown capability. **3A5-SC14**, **4A3-SC8**, and **5A2-SC8** dendrimers were formulated with Cy5.5-labeled siRNA/siFVII and injected into mice i.v. These NPs have nearly identical size, charge (ζ potential), and siRNA encapsulation efficiency in PBS (*SI Appendix*, Fig. S9 *A–C*). Their biodistribution was quantified by whole-animal and organ imaging after 24 h, and FVII activity was measured 3 d after injection. Free siRNA was primarily cleared through the kidneys, whereas **3A5-SC14**, **4A3-SC8**, and **5A2-SC8** all mediated siRNA accumulation mainly in the liver (*SI Appendix*, Fig. S9*D*). These dendrimers show varying capability to silence gene expression in hepatocytes based on dendrimer structure. **4A3-SC8** and **5A2-SC8** enabled >95% FVII knockdown at 1 mg/kg, whereas **3A5-SC14** only enabled 40% knockdown at 3 mg/kg (*SI Appendix*, Fig. S9*E*). Despite nearly identical NP physical properties and biodistribution, there was a significant difference in siRNA-mediated silencing. These data clearly show that, although most NPs localize to the liver, cell type-specific uptake and intracellular release attributes can vary greatly with different dendrimers according to chemical structure.

In Vivo Toxicity and Delivery Evaluation of Degradable Dendrimers in Mice Bearing Aggressive, *MYC*-Driven Liver Cancer. To identify degradable dendrimers with the required balance of low toxicity and high potency required for liver cancer treatment, we evaluated

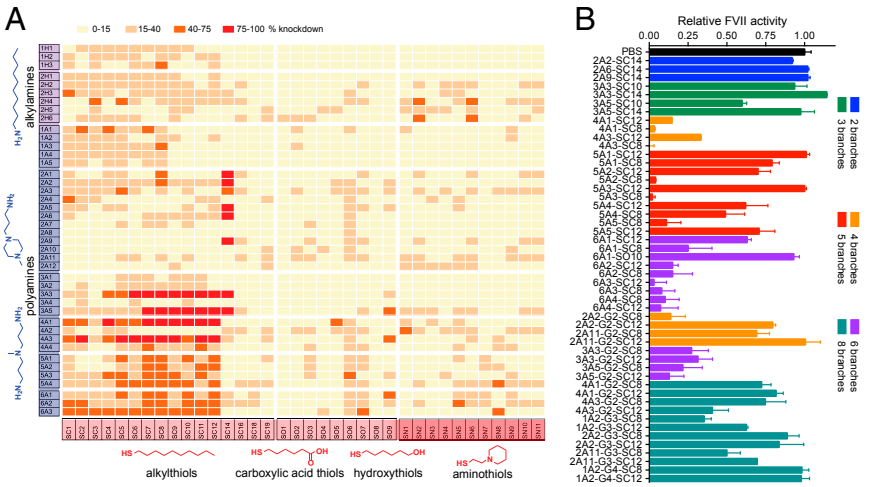

Fig. 3. Systematic in vitro and in vivo siRNA delivery analysis identified dendrimers that can overcome intracellular and extracellular delivery barriers. (*A*) A heat map of luciferase silencing in HeLa-Luc cells after treatment with dendrimer NPs (33 nM siLuc, $n = 3$) illustrates SARs (*SI Appendix*, Fig. S6). Luciferase activity and cell viability were measured to identify dendrimers that balance high delivery potency with low toxicity. (*B*) Lead G1 to G4 degradable dendrimers with diversified structures were evaluated for FVII knockdown in mice at a siRNA dosage of 1 mg/kg ($n = 3$). Data are shown as mean ± SD. This process established SAR and enabled rational design of higher generation dendrimers with predicted activity.

in vivo toxicity of the top five degradable dendrimers first in healthy wild-type mice and then in chronically ill mice bearing aggressive liver tumors. We used a clinically relevant Tet-Off *MYC* inducible transgenic liver cancer model (*SI Appendix*, Fig. S10) to provide a difficult delivery challenge that captures late-stage disease (20, 40). This model was used first to evaluate toxicity, then to examine tumor cell delivery potential, and finally for efficacy studies. Because tumors are more aggressive when *MYC* is overexpressed at earlier developmental time points, we induced *MYC* immediately after birth (day 0), which resulted in liver tumors that grow rapidly after initiation (Fig. 4*A*). About 5% of the liver is cancerous by the age of 26 d (day 26), and after an additional 2 wk, the liver becomes consumed by the disease (~75% tumor by day 40). NPs were formulated with nonimmunogenic control siRNA to best evaluate the toxicity of the individual dendrimers themselves. Size and ζ potential measurements of each NP in PBS buffer showed similar size, 64–80 nm in diameter, and near-neutral surface charge for all dendrimers (*SI Appendix*, Fig. S11). This suggests that any observed toxicity can be attributed to the individual dendrimer structures. Each formulated NP was injected i.v. into healthy mice at a 4 mg/kg control siRNA (siCTR) dose (100 mg/kg dendrimer). Body weight loss was used as a simple but informative parameter to quickly identify nontoxic dendrimers. After injection with **4A3-SC8**, mice became sick and lost nearly 20% of their weight on the first day postinjection (Fig. 4*B*). Mice injected with **4A1-SC8** and **5A3-SC8** NPs lost about 7% body weight on the first day, and the weight loss did not recover on the second day. More positively, mice injected with **5A2-SC8** and **6A3-SC12** NPs were minimally affected and gained weight normally after the first day.

Based on these results, we chose **5A2-SC8** and **6A3-SC12** for further evaluation of their in vivo toxicity in chronically ill mice bearing aggressive liver cancer with single and multiple injections. At the age of 32 d (day 32), mice with livers dispersed with tumors were injected with **5A2-SC8** or **6A3-SC12** NPs at 3 mg/kg siCTR dose (75 mg/kg dendrimer). Mice receiving **5A2-SC8** NPs were mildly affected, whereas those mice receiving **6A3-SC12** NPs maintained a 10% body weight loss and could not recover (*SI Appendix*, Fig. S12). After multiple injections, these mice died 7 d earlier compared with mice that received no treatment because of the toxicity of **6A3-SC12** carrier (Fig. 4*C*). These data show that small changes in chemical structure can produce large changes in toxicity. More significantly, it is clear that tumor-bearing mice are more sensitive to intervention than healthy mice.

To further examine toxicity, **5A2-SC8** was hydrolyzed into small-molecule byproducts (*SI Appendix*, Fig. S13). The isolated degradation products were nontoxic at relevant concentrations and possessed the same cytotoxicity profile as the intact parent **5A2-SC8** formulated NPs (*SI Appendix*, Fig. S14). **5A2-SC8** NPs were also stable in conditions designed to mimic injection, physiological, and superphysiological conditions. siRNA remained entrapped for >6 d without leakage, even in 50% serum conditions (*SI Appendix*, Fig. S15). Additionally, the NPs remained small (~80 nm) and narrowly distributed for >6 d in PBS (*SI Appendix*, Fig. S16) and for >2 d in 50% serum conditions (*SI Appendix*, Fig. S17) without aggregation. Ultimately, **5A2-SC8** emerged as an optimal degradable dendrimer with a broad therapeutic window. It was identified as potent ($EC_{50} < 0.02$ mg/kg siFVII) in dose–response experiments (Fig. 4*D*), while being well tolerated in separate toxicity studies.

Systemic Administration of a *let-7g* miRNA Mimic Inside of 5A2-SC8 NPs Enables Significant Suppression of Liver Tumor Growth. To evaluate the ability of degradable dendrimer NPs to deliver a

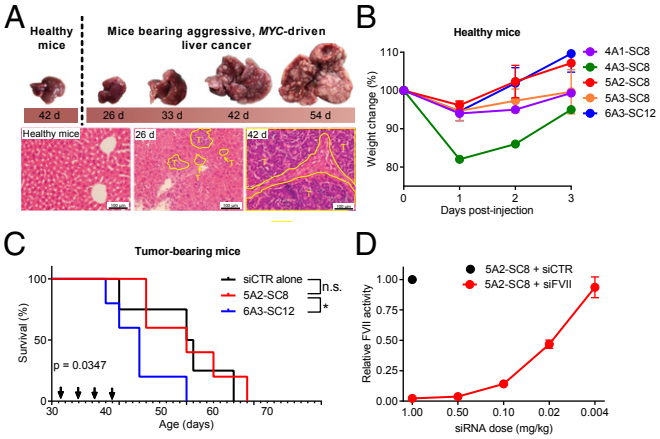

Fig. 4. Degradable dendrimers were identified that balance low toxicity and high delivery efficacy in mice bearing aggressive liver cancer. (*A*) Tumors grow rapidly after initiation in the *MYC* inducible transgenic model. All liver images are in proportional scale. The size of the liver, as well as the percentage of tumors, increases as the liver becomes consumed by the disease. White cancerous regions are visible at day 26 and progressively develop. (*B*) Wild-type, healthy mice (day 26) were injected i.v. with lead NPs at 4 mg/kg siCTR (100 mg/kg dendrimer) ($n = 3$). Body weight change varied among the formulations according to the dendrimer identity. (*C*) Kaplan–Meier survival curve of transgenic mice injected at days 32, 36, 40, and 44 with **5A2-SC8** and **6A3-SC12** NPs at 3 mg of siCTR/kg (75 mg/kg dendrimer) ($n = 5$). In tumor-bearing mice (a vulnerable host), toxicity of the carrier was exaggerated, and only **5A2-SC8** was able to be well tolerated without affecting survival (*SI Appendix*, Fig. S12). (*D*) **5A2-SC8** NPs possess an EC_{50} of 0.02 mg/kg. **5A2-SC8** encapsulating siCTR (black data point) did not result in FVII knockdown ($n = 3$). Data are shown as mean ± SD; Mantel–Cox test; n.s., $P > 0.05$; *$P < 0.05$.

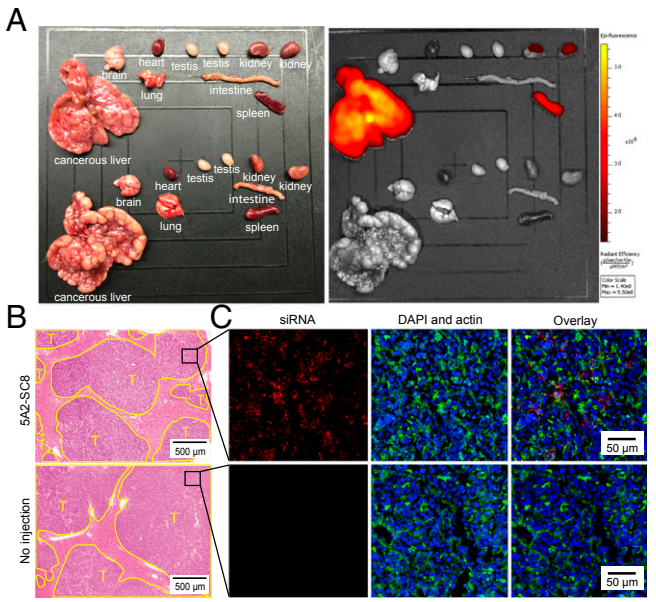

Fig. 5. Fluorescence imaging confirmed delivery of siRNA into tumor cells. (*A*) Gross anatomy and fluorescence imaging of mice bearing *MYC*-driven liver tumors (day 41) show that **5A2-SC8** NPs mediate massive siRNA accumulation in the whole cancerous liver, with minor accumulation in the spleen and kidneys 24 h after i.v. injection (1 mg/kg Cy5.5-siRNA). Tumor tissues of the liver were collected, embedded, and sectioned for H&E staining and confocal imaging 24 h after i.v. injection to further confirm delivery into tumor cells. (*B*) H&E staining confirms that the livers contain tumors. The same slides of tumor tissues were scanned using confocal imaging and captured under three channels: DAPI for nuclei (blue), FITC for phalloidin-stained actin (green), and Cy5.5 for siRNA (red). (*C*) Confocal imaging of the same region shows that **5A2-SC8** can efficiently deliver siRNA into tumor cells inside of the liver.

therapeutic miRNA mimic for liver cancer therapy, we again used the aggressive, *MYC* transgenic liver cancer model induced at day 0 (40). These mice develop rapidly growing cancers resembling pediatric hepatoblastoma (HB), a tumor type that shares many of the molecular features of HCC. Abdominal distention from mass effect was grossly visible after only 20 d. Without intervention, mice died within 60 d after birth. Given the speed and lethality of this model, there are limited opportunities for successful therapy.

We first examined whether **5A2-SC8** NPs could deliver siRNA into tumor cells. By the age of 41 d (day 41), the livers of these transgenic mice had dramatically increased in size and were full of cancerous tissues (Fig. 5*A*). On day 40, 1 mg/kg Cy5.5-labeled siRNA was administered i.v. in **5A2-SC8** NPs. At 24 h postinjection, fluorescence imaging showed **5A2-SC8** mediated siRNA accumulation in the cancerous liver, with only minor accumulation in the spleen and kidneys (Fig. 5*A*). High liver uptake of **5A2-SC8** NPs was achieved, despite cancerous livers being much larger than normal livers (*SI Appendix*, Fig. S18*A*). To further confirm that **5A2-SC8** NPs can deliver siRNA in vivo into tumor cells, tissues were collected and imaged 24 h after i.v. injection. In H&E-stained sections, small and mitotically active sheets of cells clearly delineated malignant from nonmalignant regions of the liver (*SI Appendix*, Fig. S18*B*). Confocal imaging confirmed that **5A2-SC8** NPs were able to effectively deliver labeled siRNA into tumor cells in addition to hepatocytes (Fig. 5*C*). We next verified that **5A2-SC8** NPs could enable siRNA-mediated silencing in this cancer model. After tumor development has initiated (day 26), delivery of a single dose of siFVII i.v. showed potent silencing of FVII protein using a blood assay and by quantitative PCR in harvested liver tissues (*SI Appendix*, Fig. S19 *A* and *B*).

We then evaluated the therapeutic benefit of **5A2-SC8**–mediated small-RNA delivery in these chronically ill mice. One of the most important miRNAs is *let-7*, a tumor suppressor family down-regulated in many tumor types (41, 42). Because endogenous *let-7g* is known to be down-regulated in HB and HCC (40), we wanted to test whether delivery of a *let-7g* mimic in this setting could inhibit the development of liver cancer. *Let-7g* was encapsulated in **5A2-SC8** NPs and delivered i.v. (1 mg/kg) to tumor-bearing mice (day 26). *Let-7g* expression was increased 13-fold in liver tissues 48 h postinjection (Fig. 6*A*). This experiment confirmed that **5A2-SC8** can deliver miRNA mimics to cancerous livers.

Finally, we started a therapeutic regimen from day 26 by weekly administration of **5A2-SC8** NPs containing *let-7g* mimic or control mimic (CTR) at 1 mg/kg. At day 50, the mice that received the *let-7g* mimic had grossly smaller abdomens and reduced tumor burden (Fig. 6*B*). *Let-7g* caused reduction of abdominal circumference, quantitative of tumor growth (Fig. 6*C*). The effect on tumor growth was confirmed by ex vivo liver imaging (Fig. 6*D*). Delivery of *let-7g* weekly from 26 to 61 d did not result in any significant weight change compared with control (*SI Appendix*, Fig. S20), and more importantly, the therapy significantly extended survival (Fig. 6*E*). All control mice receiving no treatment and mice receiving **5A2-SC8** NPs with CTR-mimic died around 60 d of age. Strikingly, delivery of *let-7g* using **5A2-SC8** NPs provided a dramatic survival benefit, with one mouse living to 100 d. These results show that **5A2-SC8** can balance high delivery efficacy with low toxicity in chronically ill transgenic mice to provide a significant therapeutic benefit by effective inhibition of liver tumor growth.

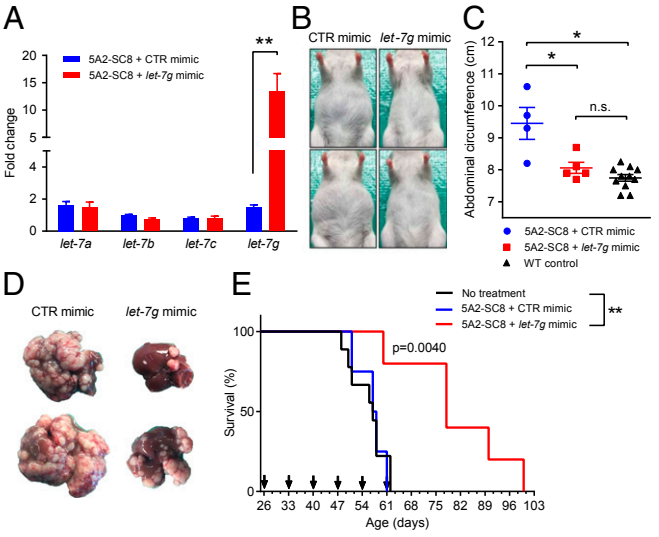

Fig. 6. Modular degradable dendrimers can deliver a therapeutic *let-7g* miRNA mimic to a clinically relevant and aggressive, *MYC*-driven genetic liver cancer model, resulting in a significant survival benefit. (*A*) **5A2-SC8** NPs enable delivery of *let-7g* to liver tissues of transgenic mice bearing *MYC*-driven liver tumors (single injection, 1 mg/kg, day 26 mice, 48 h postinjection). *Let-7g* expression was significantly increased, whereas other *let-7* family members were unaffected. (*B*) Mice bearing *MYC*-driven liver tumors were given weekly i.v. injections of 1 mg/kg *let-7g*, starting on day 26 (which is after initiation of tumor development) until day 61. Mice receiving *let-7g* had visibly smaller abdomens. (*C*) Abdominal circumference was significantly smaller for treated mice compared with controls. (*D*) Representative images of livers from *let-7g* mimic- and control mimic-injected mice show reduced tumor burden. (*E*) Weekly delivery of 1 mg/kg *let-7g* (day 26 to day 61) significantly extends survival. All control mice receiving no treatment ($n = 9$) and mice receiving **5A2-SC8** NPs ($n = 5$) containing a control untargeted mimic died around 60 d after birth. *Let-7g* mimic-treated and control groups did not exhibit any unusual weight change (*SI Appendix*, Fig. S20). Strikingly, delivery of *let-7g* inside of **5A2-SC8** NPs provided a pronounced survival benefit.

Discussion

The development of therapies that balance high potency and low toxicity is a vexing problem for cancer treatment. It is particularly challenging in liver cancer, where drug-induced hepatotoxicity exacerbates the underlying liver disease (12). Here, we generated a modular dendrimer delivery system for small RNAs that balances low toxicity and high efficacy by integrating degradability into dendrimers while simultaneously diversifying cores, peripheries, and generations to overcome multiple delivery barriers. These carriers can provide high potency in tumors without causing additional harm to normal tissues, solving a critical issue in treating aggressive liver cancer.

A number of effective in vivo siRNA carriers for hepatic gene knockdown in healthy rodents and nonhuman primates have been reported with a main focus on delivery potency (3, 4, 6, 8, 43). Existing carriers are certainly outstanding for manipulating in vivo targets but may not be able to satisfy the low toxicity requirement in late-stage cancerous livers. In 2009, it was reported that tumor growth was greatly suppressed by delivering *miR-26a* using adenoassociated viruses into a less aggressive induction of the transgenic mouse model, igniting a new hope for liver cancer treatment with miRNA therapeutics (15). In this work, we explored the critical interplay of nonviral carrier toxicity and efficacy in a clinically relevant cancer model.

This study establishes that modular degradable dendrimers are viable carriers for small-RNA delivery that achieve the goal of balanced low toxicity and high potency to effectively inhibit the growth of aggressive liver tumors. Because the therapeutic efficacy stems from a combination of a small RNA (*let-7g*) with the carrier's reduced toxicity, degradable dendrimers are excellent candidates to deliver a variety of small RNAs in translational applications in normal and cancerous tissues. For example, this will allow future manipulation of numerous genes in the liver in a time- and dose-dependent manner without concern of off-target material-induced effects. It will also be important to explore combination therapies involving siRNAs against oncogenes, miRNA tumor suppressors, and chemotherapeutic drugs to advance clinical utility. Overall, this work shows that the interface between chemical design, cancer biology, and the clinical disease setting must be carefully appreciated to develop the next generation of oligonucleotide-based cancer therapies.

Methods

Detailed materials, methods, and additional Figs. S1–S28 are provided in *SI Appendix*. This includes descriptions of dendrimer reaction optimization, synthesis, and characterization; preparation and characterization of dendrimer–RNA NPs; in vitro and in vivo gene silencing; structure–activity correlation; animal studies; and statistics.

ACKNOWLEDGMENTS. D.J.S. gratefully acknowledges financial support from the Cancer Prevention and Research Institute of Texas (CPRIT) (R1212), The Welch Foundation (I-1855), the American Cancer Society (ACS-IRG-02-196), and The Mary Kay Foundation (049-15). L.H.N. was supported by a Howard Hughes Medical Institute (HHMI) Predoctoral International Student Fellowship. J.B.M. was supported by a CPRIT Fellowship (RP140110). H.Z. was supported by the Pollack Foundation, an NIH K08 Grant (1K08CA157727), an NIH/NCI R01 Grant (1R01CA190525), a Burroughs Wellcome Career Medical Award, and CPRIT (R1209).

1. Whitehead KA, Langer R, Anderson DG (2009) Knocking down barriers: Advances in siRNA delivery. *Nat Rev Drug Discov* 8(2):129–138.
2. Kanasty R, Dorkin JR, Vegas A, Anderson D (2013) Delivery materials for siRNA therapeutics. *Nat Mater* 12(11):967–977.
3. Akinc A, et al. (2008) A combinatorial library of lipid-like materials for delivery of RNAi therapeutics. *Nat Biotechnol* 26(5):561–569.
4. Semple SC, et al. (2010) Rational design of cationic lipids for siRNA delivery. *Nat Biotechnol* 28(2):172–176.
5. Davis ME, et al. (2010) Evidence of RNAi in humans from systemically administered siRNA via targeted nanoparticles. *Nature* 464(7291):1067–1070.
6. Love KT, et al. (2010) Lipid-like materials for low-dose, in vivo gene silencing. *Proc Natl Acad Sci USA* 107(5):1864–1869.
7. Siegwart DJ, et al. (2011) Combinatorial synthesis of chemically diverse core-shell nanoparticles for intracellular delivery. *Proc Natl Acad Sci USA* 108(32):12996–13001.
8. Jayaraman M, et al. (2012) Maximizing the potency of siRNA lipid nanoparticles for hepatic gene silencing in vivo. *Angew Chem Int Ed Engl* 51(34):8529–8533.
9. Alabi CA, et al. (2013) Multiparametric approach for the evaluation of lipid nanoparticles for siRNA delivery. *Proc Natl Acad Sci USA* 110(32):12881–12886.
10. Whitehead KA, et al. (2014) Degradable lipid nanoparticles with predictable in vivo siRNA delivery activity. *Nat Commun* 5:4277.
11. Roberts LR (2008) Sorafenib in liver cancer—just the beginning. *N Engl J Med* 359(4):420–422.
12. Scudellari M (2014) Drug development: Try and try again. *Nature* 516(7529):S4–S6.
13. Ventura A, Jacks T (2009) MicroRNAs and cancer: Short RNAs go a long way. *Cell* 136(4):586–591.
14. Ladeiro Y, et al. (2008) MicroRNA profiling in hepatocellular tumors is associated with clinical features and oncogene/tumor suppressor gene mutations. *Hepatology* 47(6):1955–1963.
15. Kota J, et al. (2009) Therapeutic microRNA delivery suppresses tumorigenesis in a murine liver cancer model. *Cell* 137(6):1005–1017.
16. Kasinski AL, Slack FJ (2011) Epigenetics and genetics. MicroRNAs en route to the clinic: Progress in validating and targeting microRNAs for cancer therapy. *Nat Rev Cancer* 11(12):849–864.
17. Ling H, Fabbri M, Calin GA (2013) MicroRNAs and other non-coding RNAs as targets for anticancer drug development. *Nat Rev Drug Discov* 12(11):847–865.
18. Daige CL, et al. (2014) Systemic delivery of a miR34a mimic as a potential therapeutic for liver cancer. *Mol Cancer Ther* 13(10):2352–2360.
19. Cheng CJ, et al. (2015) MicroRNA silencing for cancer therapy targeted to the tumour microenvironment. *Nature* 518(7537):107–110.
20. Shachaf CM, et al. (2004) MYC inactivation uncovers pluripotent differentiation and tumour dormancy in hepatocellular cancer. *Nature* 431(7012):1112–1117.
21. Bosman AW, Janssen HM, Meijer EW (1999) About dendrimers: Structure, physical properties, and applications. *Chem Rev* 99(7):1665–1688.
22. Grayson SM, Fréchet JMJ (2001) Convergent dendrons and dendrimers: From synthesis to applications. *Chem Rev* 101(12):3819–3868.
23. Gillies ER, Fréchet JMJ (2002) Designing macromolecules for therapeutic applications: Polyester dendrimer-poly(ethylene oxide) "bow-tie" hybrids with tunable molecular weight and architecture. *J Am Chem Soc* 124(47):14137–14146.
24. Stiriba SE, Frey H, Haag R (2002) Dendritic polymers in biomedical applications: From potential to clinical use in diagnostics and therapy. *Angew Chem Int Ed Engl* 41(8):1329–1334.
25. Lee CC, MacKay JA, Fréchet JM, Szoka FC (2005) Designing dendrimers for biological applications. *Nat Biotechnol* 23(12):1517–1526.
26. Percec V, et al. (2010) Self-assembly of Janus dendrimers into uniform dendrimersomes and other complex architectures. *Science* 328(5981):1009–1014.
27. Kang H, DeLong R, Fisher MH, Juliano RL (2005) Tat-conjugated PAMAM dendrimers as delivery agents for antisense and siRNA oligonucleotides. *Pharm Res* 22(12):2099–2106.
28. Taratula O, et al. (2009) Surface-engineered targeted PPI dendrimer for efficient intracellular and intratumoral siRNA delivery. *J Control Release* 140(3):284–293.
29. Khan OF, et al. (2014) Ionizable amphiphilic dendrimer-based nanomaterials with alkyl-chain-substituted amines for tunable siRNA delivery to the liver endothelium in vivo. *Angew Chem Int Ed Engl* 53(52):14397–14401.
30. Wu P, et al. (2004) Efficiency and fidelity in a click-chemistry route to triazole dendrimers by the copper(I)-catalyzed ligation of azides and alkynes. *Angew Chem Int Ed Engl* 43(30):3928–3932.
31. Killops KL, Campos LM, Hawker CJ (2008) Robust, efficient, and orthogonal synthesis of dendrimers via thiol-ene "click" chemistry. *J Am Chem Soc* 130(15):5062–5064.
32. Carlmark A, Hawker C, Hult A, Malkoch M (2009) New methodologies in the construction of dendritic materials. *Chem Soc Rev* 38(2):352–362.
33. Ma X, et al. (2009) Facile synthesis of polyester dendrimers from sequential click coupling of asymmetrical monomers. *J Am Chem Soc* 131(41):14795–14803.
34. Franc G, Kakkar AK (2010) "Click" methodologies: Efficient, simple and greener routes to design dendrimers. *Chem Soc Rev* 39(5):1536–1544.
35. Wittrup A, et al. (2015) Visualizing lipid-formulated siRNA release from endosomes and target gene knockdown. *Nat Biotechnol* 33(8):870–876.
36. Schaffert D, et al. (2011) Solid-phase synthesis of sequence-defined T-, i-, and U-shape polymers for pDNA and siRNA delivery. *Angew Chem Int Ed Engl* 50(38):8986–8989.
37. Hao J, et al. (2015) Rapid synthesis of a lipocationic polyester library via ring-opening polymerization of functional valerolactones for efficacious siRNA delivery. *J Am Chem Soc* 137(29):9206–9209.
38. Anselmo AC, Mitragotri S (2014) An overview of clinical and commercial impact of drug delivery systems. *J Control Release* 190:15–28.
39. Leung AKK, et al. (2012) Lipid nanoparticles containing siRNA synthesized by microfluidic mixing exhibit an electron-dense nanostructured core. *J Phys Chem C Nanomater Interfaces* 116(34):18440–18450.
40. Nguyen LH, et al. (2014) Lin28b is sufficient to drive liver cancer and necessary for its maintenance in murine models. *Cancer Cell* 26(2):248–261.
41. Roush S, Slack FJ (2008) The let-7 family of microRNAs. *Trends Cell Biol* 18(10):505–516.
42. Boyerinas B, Park S-M, Hau A, Murmann AE, Peter ME (2010) The role of let-7 in cell differentiation and cancer. *Endocr Relat Cancer* 17(1):F19–F36.
43. Dong Y, et al. (2014) Lipopeptide nanoparticles for potent and selective siRNA delivery in rodents and nonhuman primates. *Proc Natl Acad Sci USA* 111(11):3955–3960.